

USE OF THE NEW OLCI AND SLSTR BANDS FOR ATMOSPHERIC CORRECTION OVER TURBID COASTAL AND INLAND WATERS

Kevin Ruddick and Quinten Vanhellemont

Royal Belgian Institute for Natural Sciences (RBINS), Operational Directorate for Natural Environment (ODNature), Gulledele 100, 1200. Brussels, Belgium, Email: kruddick@naturalsciences.be

ABSTRACT

The OLCI sensor has strong heritage from MERIS and some new bands, e.g. 400nm and 1020nm. The SLSTR spectral bands at 1.61 μ m and 2.25 μ m may also help improve the OLCI atmospheric correction. At 1020nm the water-leaving radiance is much lower than at shorter wavelengths and the spectral shapes of water and aerosol reflectance over the range 709-1020nm will be quite different, even in the most turbid waters. This band may therefore help improve the aerosol correction in extremely turbid waters. At 1.61 μ m and 2.25 μ m water-leaving radiance is negligible even for the most turbid waters. The advantage of these bands for atmospheric correction has been demonstrated previously for MODIS and Landsat-8. Exploiting these new bands will involve many challenges including: low signal:noise for the SWIR bands, SWIR contamination by objects at sea, straylight, calibration, OLCI/SLSTR colocation, etc.

1. INTRODUCTION

The OLCI sensor onboard Sentinel-3 has strong heritage from MERIS, but also some new bands, e.g. 400nm and 1020nm. The OLCI spectral bands are shown in Tab. 1 together with bands from SLSTR, MERIS, Sentinel-2 and the ground-based SeaPRISM instrument.

The SLSTR instrument also on S3 was designed as a follow-up to AATSR for highly accurate measurements of Sea Surface Temperature, but has spectral bands at 1.61 μ m and 2.25 μ m that may also provide information for the OLCI atmospheric correction.

The potential for using the OLCI 1020nm and SLSTR 1.61 μ m and 2.25 μ m SWIR bands arises because pure water absorption (Fig 1) is much higher at these wavelengths than at the shorter wavelengths present on MERIS. Water reflectance is thus much lower at these wavelengths, effectively zero at 1.61 μ m and 2.25 μ m and measurable at 1020nm only for extremely turbid waters [1]. This gives significant potential for distinguishing different contributions to the top of atmosphere radiance (water, surface, atmosphere) and for removing spectral ambiguities that might arise when using only visible and near infrared wavelengths.

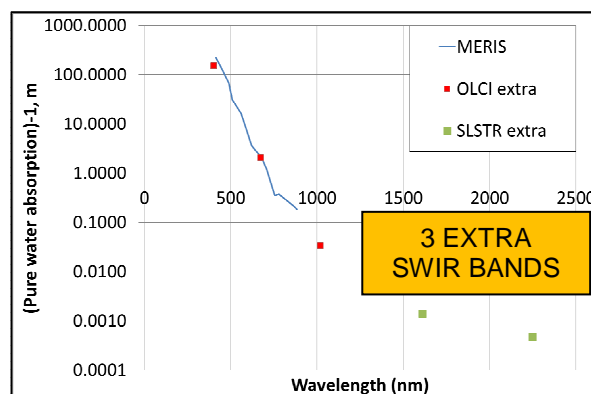


Figure 1. Inverse of pure water absorption coefficient at MERIS bands and at the extra OLCI and SLSTR bands. Data from [2] for 400-700nm and [3] for 700-2200nm.

In this paper the potential for these new bands as well as the expected challenges and difficulties will be outlined.

2. OLCI 1020nm BAND

The Remote Sensing Reflectance (R_{rs}), defined as water-leaving radiance divided by above-water downwelling radiance, has been simulated by the HYDROLIGHT radiative transfer code for non-algal particles with Suspended Particulate Matter (SPM) concentration from 1.0 to 3160.0 gm^{-3} using the same model as [4] but extended to the OLCI bands. Results in Fig. 2 show an increase in R_{rs} with increasing SPM with a shift in spectral peak to longer wavelengths. These simulated water spectra are compared with typical power law aerosol reflectance spectra in Fig. 3. For the moderately turbid waters ($SPM < 100 gm^{-3}$) the water spectra have the same shape in the near infrared [4] and have a very different spectral shape from the aerosol reflectance spectra. For extremely turbid waters ($SPM > 100 gm^{-3}$) the water reflectance spectrum flattens in the near infrared [5] until it becomes similar to the shape of aerosol reflectance (Fig. 3). This flattening will cause severe problems for turbid water atmospheric correction algorithms that calculate aerosol properties in the near infrared because water and aerosol reflectance become indistinguishable.

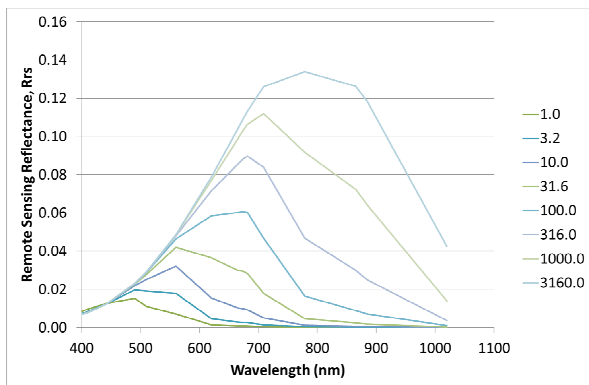


Figure 2. HYDROLIGHT simulations of (water) Remote Sensing Reflectance, R_{rs} for increasing SPM concentration (colour scale in g/m^3).

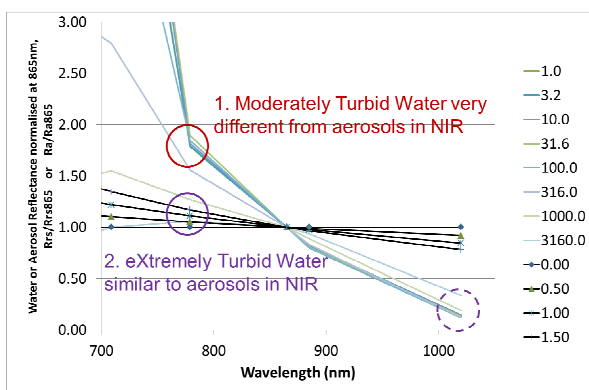


Figure 3. Simulated water (coloured lines) and typical aerosol (black lines) reflectance in near infrared normalised by magnitude at 865nm. Legend gives SPM (g/m^3) for water and Angstrom coefficient for aerosols.

A theoretical analysis of a simple two band turbid water atmospheric correction algorithm (equation A8 of [6]) shows that error increases with water reflectance at the longest wavelength, and increases as aerosol and water reflectance spectral ratios become similar. Similar conclusions are expected for more complex atmospheric correction algorithms if spectral bands with quite distinct water and aerosol properties are not used.

The OLCI 1020nm band, not currently used for the standard OLCI atmospheric correction, has a quite different spectral variation for water and aerosol reflectance (Fig. 3) and therefore has considerable potential for improving pixel-by-pixel turbid water atmospheric correction algorithms, which are notorious for failing in extremely turbid waters.

The potential use of this band for the estimation of Suspended Particulate Matter (SPM) in extremely turbid waters has also been identified [1].

3. SLSTR 1.61 μ m AND 2.25 μ m BANDS

The use of the MODIS SWIR bands has been demonstrated for improving atmospheric correction in extremely turbid waters [7], although these bands on both MODIS-TERRA and MODIS-AQUA are both very noisy and are contaminated with sensor artefacts. Much better performance has been found [8] for the Landsat-8 SWIR bands because of the significantly improved signal:noise. The SLSTR SWIR bands have similar wavelength to the Landsat-8 bands and the latter is therefore taken here as a precursor.

Fig. 4 shows Rayleigh-corrected reflectances for a Landsat-8 image in Belgian waters. Turbid waters are clearly visible at 865nm because of the non-negligible water reflectance. However, at 1.6 μ m and 2.2 μ m no turbid water effects can be seen, indicating that the water reflectance can be neglected there. At these wavelengths spatial variability is found from atmospheric effects (aerosols) as well as sea surface effects (foam, wave-breaking, fronts) and solid objects (ships, offshore constructions) [9].

The SLSTR bands should, therefore, provide much better separation between aerosol and water reflectances than the OLCI NIR bands and thus improve atmospheric correction in turbid waters.

The SLSTR data is available both for nadir and rear-views. Viewing of a target through different atmospheric paths may theoretically allow to better calculate atmospheric reflectance, although in this case the rear view will be strongly affected by “Fresnel” sky reflection at the sea surface because of the high zenith angle (55°).

4. CONCLUSIONS

OLCI is based strongly on MERIS heritage but has a few extra spectral bands plus the two additional SLSTR SWIR bands, which may significantly enhance the performance of atmospheric correction algorithms in extremely turbid waters.

4.1. Potential for the new OLCI and SLSTR bands

The OLCI 1020nm band will be useful for atmospheric correction (Fig. 2-3) in extremely turbid waters because pure water absorption is much higher at 1020nm, giving better discrimination between water and aerosols.

The SLSTR 1.61 μ m and 2.25 μ m bands will give even better discrimination between water and aerosols because water reflectance is effectively zero even in the most turbid waters. From Landsat experience (Fig 4) only atmospheric and sea surface effects will be visible in these SWIR bands.

4.2. Remaining challenges and questions

There is little experience using these new bands for ocean colour and we can expect surprises, perhaps both good and bad. For example, the high quality of the Landsat-8 SWIR bands provides significantly enhanced possibilities for atmospheric correction in extremely turbid waters compared to the MODIS SWIR bands. However, with the reduced noise level (and higher spatial resolution) new problems have been revealed such as contamination of pixels by ships and offshore structures and their wakes [9].

Challenges specific to the OLCI 1020nm band will include possible difficulties with the low signal:noise and straylight expected at this band as well as the lack of validation data for atmospheric correction algorithms.

Challenges specific to the SLSTR SWIR bands include the low signal:noise and possible impact on a SWIR-based atmospheric correction by ships, objects at sea and other surface effects [9].

The OLCI 400nm band (not studied here) may also have potential for improving atmospheric correction. At 400nm top of atmosphere radiance will be dominated by atmospheric path radiance, potentially providing a fixed point [10] for atmospheric correction. Use of data at 400nm, 412nm and 443nm might improve the estimation of Rayleigh reflectance, multiple scattering and/or the identification of absorbing aerosols.

Combination of OLCI and SLSTR data will require good co-location, intercalibration and appropriate software for efficient work.

4.3. Recommendations to ESA

Synergistic use of OLCI and SLSTR data for coastal and inland water applications requires good co-location and intercalibration of data from these instruments. It is recommended that data and/or software tools be provided to facilitate the synergistic use of co-located, radiometrically calibrated top of atmosphere OLCI and SLSTR data over coastal and inland waters.

5. ACKNOWLEDGEMENTS

This work has been carried out in the framework of the ESA CASE2X project (SEOM-DTEX-EOPS-SW-14-0002). USGS is acknowledged for Landsat-8 data. Dimitry Van Der Zande is thanked for sharing software to extend Hydrolight to the SWIR.

6. REFERENCES

1. Knaeps, E., A. I. Dogliotti, D. Raymaekers, K. Ruddick and S. Sterckx (2012). *In-situ evidence of non-zero reflectance in the OLCI 1020nm band for*

- a turbid estuary*. Remote Sensing of Environment 120: 133-144.
2. Pope, R.M. and E.S. Fry (1997). *Absorption spectrum (380–700 nm) of pure water. II. Integrating cavity measurements*, Applied Optics 36, 8710–8723.
3. Kou, L., D. Labrie and P. Chylek (1993). *Refractive indices of water and ice in the 0.65mm to 2.5mm spectral range*. Applied Optics 32: 3531–3540.
4. Ruddick, K. G., V. De Cauwer, Y. Park and G. Moore (2006). *Seaborne measurements of near infrared water-leaving reflectance - the similarity spectrum for turbid waters*. Limnology and Oceanography, 2006. 51(2): p. 1167-1179.
5. Doxaran, D., J.-M. Froidefond and P. Castaing (2003). *Remote-sensing reflectance of turbid sediment-dominated waters. Reduction of sediment type variations and changing illumination conditions effects by use of reflectance ratios*. Applied Optics 42(15): 2623-2634
6. Ruddick K., F. Ovidio & M. Rijkeboer (2000). *Atmospheric correction of SeaWiFS imagery for turbid coastal and inland waters*. Applied Optics, 39(6): p. 897–912.
7. Wang, M. and W. Shi (2005). *Estimation of ocean contribution at the MODIS near-infrared wavelengths along the east coast of the U.S.: Two case studies*. Geophysical Research Letters 32(L13606).
8. Vanhellemont, Q. and K. Ruddick (2015). *Advantages of high quality SWIR bands for ocean colour processing: examples from Landsat-8*. Remote Sensing of Environment 161: 89-106.
9. Vanhellemont, Q. and K. Ruddick (2015), *Assessment of Sentinel-3/OLCI sub-pixel variability and platform impact using Landsat-8/OLI*. Proceedings of Sentinel-3 for Science workshop held in Venice, June 2015, ESA SP -734.
10. He, X., Y. Bai, D. Pan, J. Tang and D. Wang (2012). *Atmospheric correction of satellite ocean color imagery using the ultraviolet wavelength for highly turbid waters*. Optics Express 20(18): 20754-20770.
11. Zibordi, G., B. Holben, I. Slutsker, D. Giles, D. D'Alimonte, F. Mélin, J.-F. Berthon, D. Vandemark, H. Feng, G. Schuster, E. E. Fabbri, S. Kaitala and J. Seppälä (2009). *AERONET-OC: A network for the validation of ocean color primary product*. Journal of Atmospheric and Oceanic Technology 26: 1634-1651.

Table 1. Central wavelength and width of OLCI spectral channels. OLCI bands marked in grey are not available as level 2 radiometric products. Spectral bands with central wavelength different from OLCI by more than 5nm are given in italics. MERIS bands given as “Y” are supposed equivalent to the corresponding OLCI band. Following definitions are used to group spectral ranges: visible (VIS: 400-700nm), near infrared (700-1000nm), short wave infrared (SWIR: 1-3 μ m), thermal infrared (TIR: 3 μ m-14 μ m). The “new” bands present on Sentinel-3 thought to have potential for enhanced ocean colour products are highlighted in red, bold face. Sentinel-2 (S2) wavelengths are given, although it is noted that these have much lower signal:noise. Wavelengths of the SEAPRISM ground-based instrument used for the AERONET-OC validation network [11] are also given to indicate the potential for validation of the various OLCI wavelengths. Sources consulted on 11.5.2015:

<https://sentinel.esa.int/web/sentinel/user-guides/sentinel-3-olci/resolutions/radiometric>

<https://sentinel.esa.int/web/sentinel/user-guides/sentinel-3-slstr/resolutions/radiometric>

<https://sentinel.esa.int/web/sentinel/user-guides/sentinel-2-msi/resolutions/radiometric>

	OLCI band	OLCI centre (nm)	OLCI width (nm)	SLSTR centre/width (nm)	MERIS centre/w idth (nm)	S2 centre/width (nm)	SeaPRISM centre/width (nm)
VIS	Oa1	400	15	-	-	-	-
	Oa2	412.5	10	-	Y	-	412
	Oa3	442.5	10	-	Y	443/20	443
	Oa4	490	10	-	Y	490/65	488
	Oa5	510	10	-	Y	-	-
	Oa6	560	10	555 / 20	Y	560/35	<i>551</i>
	Oa7	620	10	-	Y	-	-
	Oa8	665	10	<i>659 / 20</i>	Y	665/30	667
	Oa9	673.75	7.5	-	-	-	-
	Oa10	681.25	7.5	-	Y	-	-
NIR	Oa11	708.75	10	-	Y	705/15	-
	Oa12	753.75	7.5	-	Y	740/15	-
	Oa13	761.25	2.5	-	Y	-	-
	Oa14	764.375	3.75	-	-	-	-
	Oa15	767.5	2.5	-	-	-	-
	Oa16	778.75	15	-	Y	783/20	-
	Oa17	865	20	865 / 20	Y	865/20	870
	Oa18	885	10	-	Y	-	-
	Oa19	900	10	-	Y	-	-
	Oa20	940	20	-	-	945/20	(940)
SWIR	Oa21	1 020	40	-	-	-	1020
				1 375 / 15	-	1 375/30	-
				1 610 / 60	-	1 610/90	-
				2 250 / 50	-	2 190/180	-
TIR/Other			+ 5*TIR	-	+ 842/115	+531	

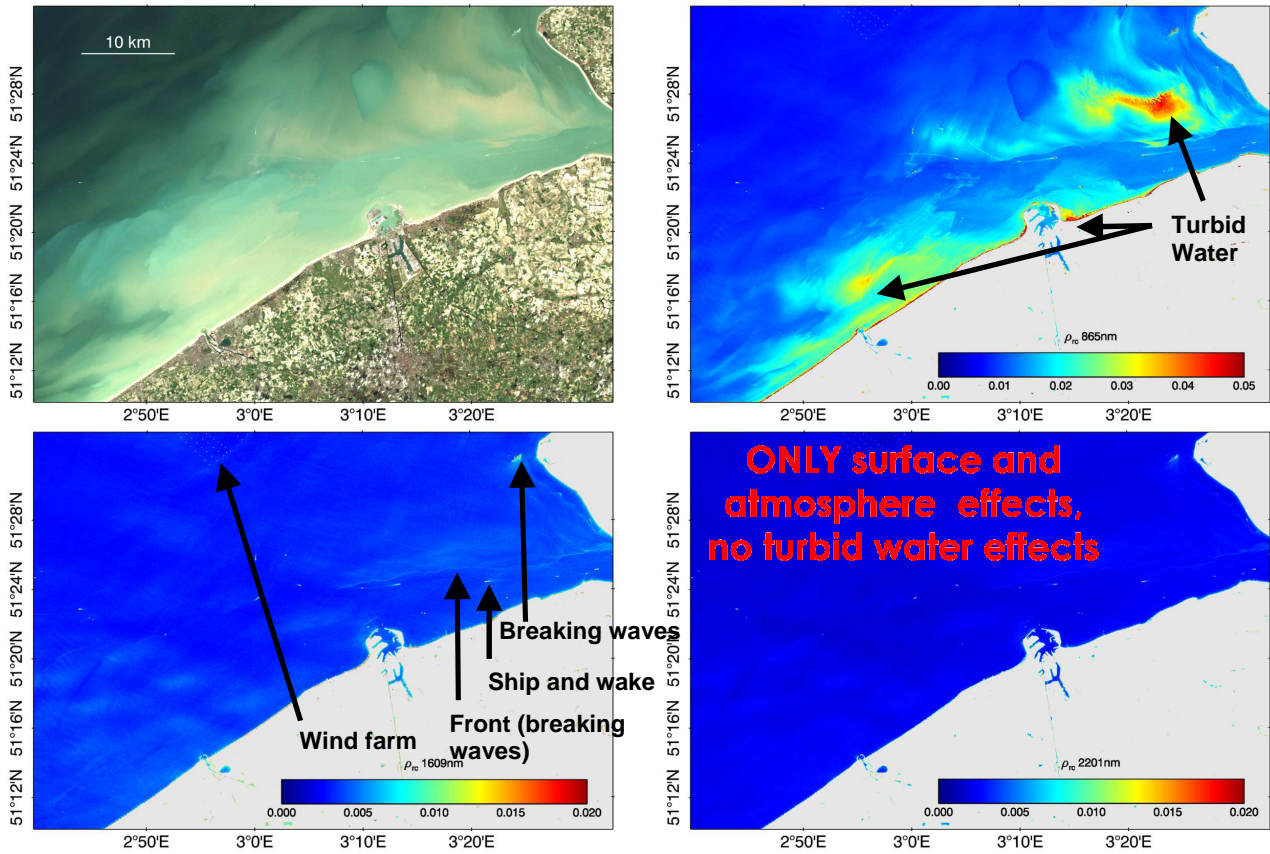


Figure 4. Landsat-8/OLI scene of Belgian coastal waters on 2014-03-16. Rayleigh corrected (a) RGB, bands 4-3-2, reflectance at (b) 865 nm, and (c) 1609nm and (d) 2201nm. ACOLITE processing [8].